JOURNAL OF MECHANICS OF CONTINUA AND MATHEMATICAL SCIENCES
www.journalimcms.org

ISSN (Online) : 2454 -7190 Vol.-17, No.-5, May (2022) pp 24-42 ISSN (Print) 0973-8975

NUMERICAL STUDY OF THE INFLUENCE OF TEMPERATURE-DEPENDENT VISCOSITY ON THE UNSTEADY LAMINAR FLOW AND HEAT TRANSFER OF A VISCOUS INCOMPRESSIBLE FLUID DUE TO A ROTATING DISC

Akter Hossain[1], Sarder Firoz Ahmmed[2]

[1]Department of Mathematical and Physical Sciences, Faculty of Sciences and Engineering, East-West University, Aftabnagar, Dhaka-1212, Bangladesh

[2] Mathematics Discipline, Khulna University, Khulna- 9208, Bangladesh

[1] akter.hossain@ewubd.edu, aakterh@yahoo.com, [2]sfahmmed@math.ku.ac.bd, sfahmmed@yahoo.com,

Corresponding Author: **Akter Hossain**

https://doi.org/10.26782/jmcms.2022.05.00003

Abstract

In this article, the effect of temperature-dependent viscosity (TVD) *on the unsteady laminar flow and heat transfer* (HT) *of a viscous incompressible fluid due to a rotating disc* (RD) *has been investigated numerically by exploiting an in-house numerical code. A set of time-dependent, axisymmetric, and non-linear partial differential equations which govern the fluid flows and heat transfer are reduced to non-linear local non-similarity ordinary differential equations by introducing a newly developed group of transformations for different time regimes. Three different solution methods, such as, (i) perturbation solution method for small* τ*, (ii) asymptotic solution method for large* τ*, and (iii) implicit finite difference method for the entire* τ *regime, have been applied to solve the resulting equations treating* τ *as the time-dependent rotating parameter. The local radial skin friction, tangential skin friction and the heat transfer are computed at the surface of the disc for different numerical parameters, such as, Prandtl number, Pr and the viscosity-variation parameter,* ε*. Besides, the key dimensionless quantities such as velocity and temperature profiles, which are inherently linked with the boundary layer thickness, are presented graphically for different values of* ε *while* $Pr = 0.72$*. It is found that the dimensionless radial, tangential and axial velocity profiles decrease as* ε *increases, and consequently, the momentum boundary layer thickness is decreased. On the other hand, the non-dimensional temperature profiles are increased owing to the increasing values of* ε*, and this effect eventually leads to a small increment in the thermal boundary layer thickness.*

Keywords: Unsteady flow, heat transfer (HT), temperature-dependent viscosity (TDV), laminar flow, and rotating disc (RD).

I. Introduction

The *rotating disc* (RD) systems are extensively used in various engineering and industrial applications such as gas turbine engines, aircraft engines, centrifugal pump systems, rotor-stator systems, computer disc drives, electronic devices, oil and food processing technologies, etc. [I], [IX],[XIV], [XXVI] . The RD-driven fluid flow is one of the most classical problems in fluid mechanics [XXVIII], which has both theoretical and practical values. Since the *heat transfer* (HT) processes in RD systems are intrinsically related to the local fluid flow traits, this feature is then coupled with the centrifugal force and 3D effect of fluid flows, and consequently, it poses serious challenges to theorists and experimentalists [V]. Hence, in-depth knowledge about local flow fields and their influence on HT processes is essential to be understood precisely. It is also extremely important and relevant for operating and designing various rotary machinery [XIII], [XVI].

The first scientist who formulated and analyzed the RD-induced fluid flow problem was Von-Ka′rma′n [XXX], and after his pioneering work, a huge research has been accomplished. However, only those works that are closely related to the present study have been introduced here. Cochran [XXXV] obtained much better results by using the patching technique for series expansions. Cochran's [XXXV] solutions have been improved by Benton [III]. Later, many researchers [XXXIV], [XVII], [XI], [VI], [VII] have studied RD-related fluid flow problems. The HT from an isothermal RD to the fluid flow has been investigated for arbitrary Prandtl number (*Pr*) by Sparrow and Gregg [IV] and for fixed *Pr* by Ostrach and Thornton [XXVII]. The HT from a non-isothermal RD in still air has been examined by Hartnett [X] using a power-law distribution of surface-temperature. The HT from a non-isothermal RD to fluids has been investigated by Awad [XXI] for various *Pr* using asymptotic analysis. Since the RD driven flow and HT have diverse practical applications, it has been observed recently that the researchers have been attempting to explore the RD induced flow and HT adopting various geometrical and physical aspects such as disc's surface roughness, extendable and stretchable discs, nanofluid, the effect of hall current, and chemical reaction. Imayama *et al.* [XXIX] have examined experimentally the effect of *disc surface roughness* on boundary-layer flow caused by RD. The joule heating and viscous dissipation effects on the flow of *nanomaterials* due to RD have been studied by Hayat *et al*. [XXXIII]. Shamshuddin *et al.* [XXII] have explored numerically the HT and viscous flow due to an *extendable* RD. The effect of *hall current* on radiative *nanofluid* flow over a RD has been studied by Nilankush *et al.* [II]. The unsteady flow of viscous fluid along with heat and mass transfer owing to a *stretchable* RD has been analyzed numerically by Ibrahim *et al.* [XXIII]. Very recently, the effect of chemical reactions on a nanofluid flow due to a RD under a magnetic field has been examined numerically by Ramzan *et al.* [XXIV].

As summarized above; it is found that the fluid viscosity was considered as constant. However, it is well-known that the thermophysical properties of the fluid generally change significantly depending on the local temperature field. Therefore, it is indispensable to consider the effect of the *temperature-dependent viscosity* (TVD) variation to predict the flow characteristics accurately. This is the motivation for our work.

However, the TDV effect has been examined by Kafoussias *et al*. [XXV], and Hossain and Munir [XVIII] for mixed convection- and by Hossain *et al.* [XX] for natural convection-flow. Later, the combined effect of a magnetic field and TDV on the unsteady flow and HT due to a RD has been investigated by Hossain *et al*. [XIX], where the physical scenario was quite complicated in the presence of the transverse magnetic field. But, a much simpler flow situation is physically desirable to look into the role of local TDV on the fluid flow and HT processes. Therefore, this article examines the influence of local TDV on the transient fluid flow and HT processes due to a RD in the absence of any *external agents* (i.e., magnetic field, electric field).

II. Description of Mathematical Formulation

The three-dimensional (3D) unsteady motion of a homogeneous incompressible viscous fluid and heat transfer due to an infinite rotating disc has been examined numerically using an in-house numerical code. It is considered that the extent of fluid is infinite in the positive *z* direction and the viscosity varies on the local temperature of the fluid. It is assumed that the disc rotates with uniform angular velocity, Ω and the disc is kept at $z = 0$, where *z* is the vertical axis of the cylindrical coordinate system where *r* and ϕ are the radial and tangential axes, respectively. The surface temperature

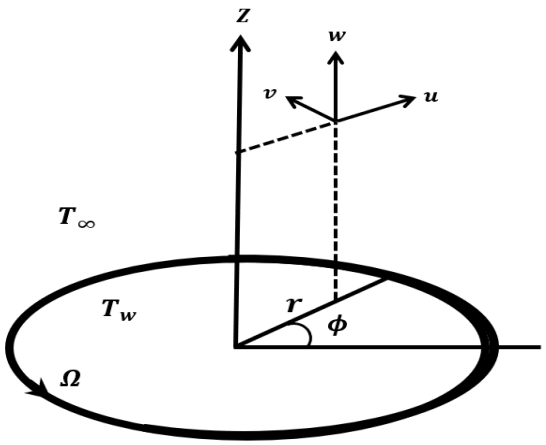

Fig. 1. The schematic view of flow configuration and the coordinate system

of the disc is maintained uniform at T_w while the ambient temperature of the fluid is kept at T_{∞}. A thin viscous layer develops in the vicinity of the surface of the disc owing to the rotation of the disc in the presence of viscous fluid, and the fluid is thrown radially outwards due to the existence of the centrifugal forces.

Figure 1 represents the flow configuration and the coordinate system of the present problem. Due to the axial symmetry, a set of partial differential equations which govern the fluid flows and heat transfer processes under the rotating disc system can be written as follows:

$$\frac{\partial u}{\partial r}+\frac{u}{r}+\frac{\partial w}{\partial z}=0 \tag{1}$$

$$\rho_\infty\left(\frac{\partial u}{\partial t}+u\frac{\partial u}{\partial r}+w\frac{\partial u}{\partial z}-\frac{v^2}{r}\right) = -\frac{\partial p}{\partial r}+\frac{\partial}{\partial r}\left[2\mu\left(\frac{\partial u}{\partial r}\right)\right]+\frac{\partial}{\partial z}\left[\mu\left(\frac{\partial u}{\partial z}+\frac{\partial w}{\partial r}\right)\right] +\frac{2\mu}{r}\left(\frac{\partial u}{\partial r}-\frac{u}{r}\right) \tag{2}$$

$$\rho_\infty\left(\frac{\partial v}{\partial t}+u\frac{\partial v}{\partial r}+\frac{uv}{r}+w\frac{\partial v}{\partial z}\right) = \frac{\partial}{\partial z}\left[\mu\left(\frac{\partial v}{\partial z}\right)\right]+\frac{\partial}{\partial r}\left[\mu\left(\frac{\partial v}{\partial r}-\frac{v}{r}\right)\right]+\frac{2\mu}{r}\left(\frac{\partial v}{\partial r}-\frac{v}{r}\right) \tag{3}$$

$$\rho_\infty\left(\frac{\partial w}{\partial t}+u\frac{\partial w}{\partial r}+w\frac{\partial w}{\partial z}\right)=-\frac{\partial p}{\partial z}+\frac{\partial}{\partial z}\left[2\mu\left(\frac{\partial w}{\partial z}\right)\right]+\frac{1}{r}\frac{\partial}{\partial r}\left[\mu r\left(\frac{\partial u}{\partial z}+\frac{\partial w}{\partial r}\right)\right] \tag{4}$$

$$\rho_\infty C_p\left(\frac{\partial T}{\partial t}+u\frac{\partial T}{\partial r}+w\frac{\partial T}{\partial z}\right)=\kappa\left(\frac{\partial^2 T}{\partial r^2}+\frac{1}{r}\frac{\partial T}{\partial r}+\frac{\partial^2 T}{\partial z^2}\right) \tag{5}$$

where u, v, and w are the radial, tangential, and axial velocity components of the fluid flow in the directions of the r, ϕ and z coordinates, respectively; p is the pressure, ρ_∞ is the fluid density, κ is the thermal conductivity of the fluid, C_p is the specific heat at constant pressure, and μ is the viscosity of the fluid. In this study, the viscosity depends on local fluid temperature, i.e., $\mu = \mu_\infty/\{1+\alpha(T-T_\infty)\}$ as applied in [XIX], which was originally developed by Ling and Libby [XV]. It should be noted here that all other physical properties associated with this study, such as the fluid density ρ_∞, the thermal conductivity of the fluid κ, and the pressure in the flow region p, are treated as constant.

The initial and boundary conditions for the flow field driven by the rotating disc, which is started impulsively with the uniform angular velocity Ω, are given below:

$$\begin{aligned}&\text{At } t=0: u=\ \text{v}=\ w=0\\ &\text{At } t>0: \begin{cases}u,w=0,\ v=r\Omega, T=T_w \text{ at } z=0\\ u,v\to 0,\ T=T_\infty, p\to 0 \text{ as } z\to\infty\end{cases}\end{aligned} \tag{6}$$

To obtain the solutions of the above-stated governing equations, at first, these equations are transformed into a convenient form using appropriate transformations. Considering the aforesaid fact in our mind, we have formulated a new set of transformations by adopting dimensional analysis for this investigation, and it is presented as follows:

$$u=r\Omega erf(\lambda\tau)\ f(\eta\ ,\tau)\ ,\ v=r\Omega g(\eta\ ,\tau)$$
$$w=-4(\nu\Omega)^{1/2}\left(erf(\lambda\tau)\right)^{3/2}h(\eta\ ,\tau),\quad \frac{T-T_\infty}{T_w-T_\infty}=\theta(\eta\ ,\tau)$$

$$\eta = \frac{1}{2}\sqrt{\left(\frac{\Omega}{\nu}\right)}\left(erf(\lambda\tau)\right)^{-1/2} z,\ \tau = \Omega t \quad \text{and } \lambda = \frac{\sqrt{\pi}}{2}$$

$$p = 2\rho_\infty \nu \Omega erf(\lambda\tau)\bar{p}(\eta,\tau) \tag{7}$$

The governing equations (1) to (5) are transformed into the following non-similarity equations after introducing the transformations as presented in (7):

$$(1+\varepsilon\theta)h''' - \varepsilon\theta' h'' - (1+\varepsilon\theta)^2\left\{4e^{-\lambda^2\tau^2}h' - 2\eta e^{-\lambda^2\tau^2}h''\right.$$

$$\left. +4erf(\lambda\tau)\frac{\partial h'}{\partial\tau} + 4\left(erf(\lambda\tau)\right)^2 h'^2 - 8\left(erf(\lambda\tau)\right)^2 hh'' - 4g^2\right\} = 0 \tag{8}$$

$$(1+\varepsilon\theta)g'' - \varepsilon\theta' g' + (1+\varepsilon\theta)^2\left\{2\eta e^{-\lambda^2\tau^2}g' - 4erf(\lambda\tau)\frac{\partial g}{\partial\tau}\right.$$

$$\left. -8\left(erf(\lambda\tau)\right)^2 h'g + 8\left(erf(\lambda\tau)\right)^2 hg'\right\} = 0 \tag{9}$$

$$\bar{p}' = (1+\varepsilon\theta)^{-1}h'' - 2\varepsilon(1+\varepsilon\theta)^{-2}\theta' h' - 6e^{-\lambda^2\tau^2}h + 2\eta e^{-\lambda^2\tau^2}h' - 4erf(\lambda\tau)\frac{\partial h}{\partial\tau} + 8\left(erf(\lambda\tau)\right)^2 hh' \tag{10}$$

$$\frac{1}{Pr}\theta'' + 2\eta e^{-\lambda^2\tau^2}\theta' + 8\left(erf(\lambda\tau)\right)^2\theta' h = 4erf(\lambda\tau)\frac{\partial\theta}{\partial\tau} \tag{11}$$

The boundary conditions for the above equation are as follows:

$$h(0,\tau) = h'(0,\tau) = 0,\ g(0,\tau) = 1,\ \theta(0,\tau) = 1$$
$$h'(\infty,\tau) = g(\infty,\tau) = \theta(\infty,\tau) = \bar{p}(\infty,\tau) = 0 \tag{12}$$

where *Pr* (= $\mu_\infty C_p/\kappa$) is the Prandtl number, and the viscosity variation parameter is defined by ε (=$\alpha(T_w - T_\infty)$). In the above equations, the prime denotes the differentiation concerning η, and this convention is valid in the subsequent sections of this article.

III. All Time Solution

To solve the system of equations (8) to (11) subject to the boundary conditions (12), we have applied an implicit finite difference method with Keller-Box [VIII] elimination technique following Hossain *et al*. [XIX] as it is found to very efficient, accurate, and widely used by Cebici and Bradshaw [XXXII], and Hossain *et al.* [XVIII], [XX]. According to the above method, as explained by Hossain *et al.* [XIX], at first, a set of governing partial differential equations is converted to a system of seven first-order ordinary differential equations where the derivatives are taken concerning η, a new variable as defined in equation (7). The converted system is then put into a finite difference scheme where the final non-linear difference equations are linearized by using Newton's quasi-linearization method. Finally, the resulting linear difference equations are solved by using the block-tridiagonal factorization method developed by Keller [VIII]. The numerical solutions are obtained in this study over a range for $\tau \in [0, 50]$. It is found that our selection for $\tau_{\max} = 50$ is reasonable to get the corresponding asymptotic solution of the functions for the large τ as discussed in the following section: **V**.

The important physical quantities of interest in this study are the tangential shear stress, radial shear stress, and heat flux from the disc surface, and these quantities are calculated by using the following formulae at the surface of the disc. To find the tangential shear stress, τ_t, and the radial shear stress, τ_r, we have applied Newtonian formulae under the cylindrical coordinate system as given below:

$$\tau_t = \left[\mu\left(\frac{\partial v}{\partial z} + \frac{1}{r}\frac{\partial w}{\partial \varphi}\right)\right]_{z=0} \tag{13}$$

$$\tau_r = \left[\mu\left(\frac{\partial u}{\partial z} + \frac{\partial w}{\partial r}\right)\right]_{z=0} \tag{14}$$

The heat flux from the disc surface to the fluid is calculated by using the well-known Fourier's law for heat conduction as presented below:

$$q = -k\left(\frac{\partial T}{\partial z}\right)_{z=0} \tag{15}$$

One can easily calculate the values of the dimensionless radial skin-friction, tangential skin-friction, as well as the rate of heat transfer from the following relations, which are obtained by using the transformations as presented in (7), after knowing the values of the functions h, g and θ, and their derivatives from the numerical computations:

$$\bar{\tau}_r(1+\varepsilon) = \left(erf(\lambda\tau)\right)^{1/2} h''(0,\tau), \bar{\tau}_t(1+\varepsilon) = \left(erf(\lambda\tau)\right)^{-1/2} g'(0,\tau)$$
$$\bar{q} = -\left(erf(\lambda\tau)\right)^{-1/2}\theta'(0,\tau) \tag{16}$$

where $\bar{\tau}_r = \frac{2\nu^{1/2}}{r\mu_\infty \Omega^{3/2}}\tau_r$, $\bar{\tau}_t = \frac{2\nu^{1/2}}{r\mu_\infty \Omega^{3/2}}\tau_t$ and $\bar{q} = \frac{2}{\kappa(T_w - T_\infty)}\sqrt{\frac{\nu}{\Omega}}q$

IV. Small Time Solution

If we take τ is small i.e., $\tau << 1$, then the transformations given in (7) reduce to the following forms, which are valid for small-time regime.

$$u = r\Omega\tau\, f(\eta,\tau),\ v = r\Omega g(\eta,\tau)$$
$$w = -4(\nu\Omega)^{1/2}\tau^{3/2}h(\eta,\tau),\quad \frac{T - T_\infty}{T_w - T_\infty} = \theta(\eta,\tau)$$
$$\eta = \frac{1}{2}\sqrt{\left(\frac{\Omega}{\nu\tau}\right)}z,\ \tau = \Omega t,\qquad p = 2\rho_\infty \nu\Omega\tau\bar{p}(\eta,\tau) \tag{17}$$

Therefore, after the utilization of the above transformations, the governing equations (1) to (5) take the following forms:

$$(1+\varepsilon\theta)h''' - \varepsilon h''\theta'$$
$$= (1+\varepsilon\theta)^2\left(4h' - 2\eta h'' + 4\tau^2 h'^2 - 8\tau^2 h''h - 4g^2 + 4\tau\frac{\partial h'}{\partial \tau}\right) \tag{18}$$

$$(1+\varepsilon\theta)g'' - \varepsilon g'\theta' = (1+\varepsilon\theta)^2\left(8\tau^2 h'g - 2\eta g' - 8\tau^2 hg' + 4\tau\frac{\partial g}{\partial\tau}\right) \quad (19)$$

$$\bar{p}' = (1+\varepsilon\theta)^{-1}h'' - 2\varepsilon(1+\varepsilon\theta)^{-2}\theta' h' - 6h + 2\eta h' - 4\tau\frac{\partial h}{\partial\tau} + 8\tau^2 hh' \quad (20)$$

$$\frac{1}{Pr}\theta'' + 2\eta\theta' + 8\tau^2\theta' h = 4\tau\frac{\partial\theta}{\partial\tau} \quad (21)$$

The corresponding boundary conditions can be written as follows

$$h(0,\tau) = h'(0,\tau) = 0,\ g(0,\tau) = 1,\ \theta(0,\tau) = 1$$
$$h'(\infty,\tau) = g(\infty,\tau) = \theta(\infty,\tau) = \bar{p}(\infty,\tau) = 0 \quad (22)$$

It is clear that the equations (18) to (21) are non-similar and parabolic partial differential equations. Since the above equations are obtained under the assumption of a small τ limit, i.e., τ<<1, we can obtain the solutions of the equations (18) to (21) by applying the perturbation technique treating τ as a perturbation parameter. Hence, the functions *h*, *g*, and θ can be written as follows:

$$h(\eta,\tau) = \sum_{i=0}^{\infty}\tau^{2i}h_i(\eta),\ g(\eta,\tau) = \sum_{i=0}^{\infty}\tau^{2i}g_i(\eta)\ \text{ and } \theta(\eta,\tau) = \sum_{i=0}^{\infty}\tau^{2i}\theta_i(\eta) \quad (23)$$

where $h_i(\eta)$, $g_i(\eta)$ and $\theta_i(\eta)$ are the functions of η only.

After adopting the above expressions as demonstrated in (23), the following equations can be obtained from the equations (18), (19), and (21) when the terms are taken from series solutions only up to $O(\tau^4)$.

$$(1+\varepsilon\theta_0)h'''_0 - \varepsilon h'_0\theta'_0 = (1+\varepsilon\theta_0)^2\left(4h'_0 - 2\eta h''_0 - 4g_0^2\right) \quad (24)$$

$$(1+\varepsilon\theta_0)g''_0 = \varepsilon g'_0\theta'_0 - 2\eta(1+\varepsilon\theta_0)^2 g'_0 \quad (25)$$

$$\frac{1}{Pr}\theta''_0 + 2\eta\theta'_0 = 0 \quad (26)$$

$$h_0(0) = h'_0(0) = 0, g_0(0) = \theta_0(0) = 1$$
$$h'_0(\infty) = 0, g_0(\infty) = \theta_0(\infty) = 0 \quad (27)$$

$$(1+\varepsilon\theta_0)h'''_1 + \varepsilon\left(\theta_1 h'''_0 - h''_0\theta'_1 - h''_1\theta'_0\right) - (1+\varepsilon\theta_0)^2\left(12h'_1 + 4h'^2_0 - 8h''_0 h_0 - 8g_0 g_1 - 2\eta h''_1\right) - 2\varepsilon\theta_1(1+\varepsilon\theta_0)\left(4h'_0 - 2\eta h''_0 - 4g_0^2\right) = 0 \quad (28)$$

$$(1+\varepsilon\theta_0)g''_1 + \varepsilon\left(\theta_1 g''_0 - g'_0\theta'_1 - g'_1\theta'_0\right) - (1+\varepsilon\theta_0)^2\left(8g_1 + 8h'_0 g_0 - 8g'_0 h_0 - 2\eta g'_1\right) + 4\varepsilon\eta\theta_1(1+\varepsilon\theta_0)g'_0 = 0 \quad (29)$$

$$\frac{1}{Pr}\theta''_1 + 2\eta\theta'_1 - 8\theta_1 = -8h_0\theta'_0$$
$$h_1(0) = h'_1(0) = 0, g_1(0) = \theta_1(0) = 0$$
$$h'_1(\infty) = 0, g_1(\infty) = \theta_1(\infty) = 0 \quad (30)$$

$$(1+\varepsilon\theta_0)h'''_2 + \varepsilon\left(\theta_2 h'''_0 + \theta_1 h'''_1 - h''_0\theta'_2 - h''_1\theta'_1 - h''_2\theta'_0\right)$$
$$-(1+\varepsilon\theta_0)^2\left(20h'_2 + 8h'_0h'_1 - 8h''_0h_1 - 8h''_1h_0 - 2\eta h''_2 - 8g_0g_2 - 4{g_1}^2\right)$$
$$-2\varepsilon\theta_1(1+\varepsilon\theta_0)\left(12h'_1 - 2\eta h''_1 - 8h''_0h_0 - 8g_0g_1 + 4{h'_0}^2\right)$$
$$-\varepsilon\{2\theta_2 + \varepsilon\left(2\theta_0\theta_2 + {\theta_1}^2\right)\}\left(4h'_0 - 2\eta h''_0 - 4g_0^2\right) = 0 \quad (31)$$

$$(1+\varepsilon\theta_0)g''_2 + \varepsilon\left(\theta_2 g''_0 + \theta_1 g''_1 - g'_0\theta'_2 - g'_1\theta'_1 - g'_2\theta'_0\right)$$
$$-(1+\varepsilon\theta_0)^2\left(16g_2 + 8h'_0g_1 + 8h'_1g_0 - 8g'_0h_1 - 8g'_1h_0 - 2\eta g'_2\right)$$
$$-2\varepsilon\theta_1(1+\varepsilon\theta_0)\left(8g_1 + 8h'_0g_0 - 8g'_0h_0 - 2\eta g'_1\right)$$
$$+2\eta\varepsilon\{2\theta_2 + \varepsilon\left(2\theta_0\theta_2 + {\theta_1}^2\right)\}g'_0 = 0 \quad (32)$$

$$\frac{1}{Pr}\theta''_2 + 2\eta\theta'_2 - 16\theta_2 = -8\left(h_0\theta'_1 + h_1\theta'_0\right) \quad (33)$$

$$h_2(0) = h'_2(0) = 0, g_2(0) = \theta_2(0) = 0$$
$$h'_2(\infty) = 0, g_2(\infty) = \theta_2(\infty) = 0 \quad (34)$$

It is indubitable that the equations (24) and (25) are coupled and non-linear differential equations by nature, and hence the analytical solution of these equations is not possible in the presence of $\varepsilon \neq 0.0$ (i. e., the viscosity of the fluid varies with temperature field), and hence one can easily find the same characteristics for the subsequent sets of equations. Therefore, a numerical method is required to solve the above-mentioned equations. Thus, in this study, we have applied the Nachtsheim-Swigert iteration [XXVI] techniques along with the sixth-order implicit Runge-Kutta-Butcher [XII] method to find the numerical solutions of equations (24) to (27). The above-mentioned method has also been applied to obtain the solutions for the subsequent set of equations (28) to (34) for different values of pertinent parameters.

Once the above-mentioned numerical method has been implemented successfully, the values of the functions h_n, g_n, and θ_n for n = 0,1,2,… and their derivatives can be found easily. Therefore, the values of dimensionless radial-skin friction, tangential skin friction as well as the heat transfer rate can be calculated from the equation (16) subject to a small τ limit and the resulting form of the above-mentioned quantities can be written as follows:

$$\bar{\tau}_r(1+\varepsilon) = \tau^{1/2}h''(0,\tau), \bar{\tau}_t(1+\varepsilon) = \tau^{-1/2}g'(0,\tau)$$
$$\bar{q} = -\tau^{-1/2}\theta'(0,\tau) \quad (35)$$

With the aim of validation of our results, we have computed the dimensionless tangential skin friction from the equation (35) by using the series expansion as presented in (23). If we take the terms up to the third order, then we have obtained an expression as shown in (36) using the term 'Present'. Finally, our obtained expression has been compared with the same quantity as derived by Benton [III] as follows:

$$(1+\varepsilon)\bar{\tau}_t = \begin{cases} -1.13009\,\tau^{-1/2} - 0.18790\,\tau^{3/2} + 0.011749\,\tau^{7/2} & \text{'Present'} \\ -1.128\,\tau^{-1/2} - 0.1884\,\tau^{3/2} + 0.011759\,\tau^{7/2} & \text{Benton [III]} \end{cases} \quad (36)$$

Hence, one can easily conclude from equation (36) that the two expressions are in excellent agreement, which also confirms that our newly developed transformations as presented in (7) are reasonably accurate. Hence, one can easily expect that our transformations will also be suitable for the large-time regime, and the all-time regime under rotating disc systems, which will be discussed in the subsequent sections.

V. Large time solution

If $\tau >> 1$ i.e., for large time, then the transformations as presented in (7) take the following forms, which are valid for large time regime:

$$u = r\Omega f(\eta\ ,\tau)\ ,\ v = r\Omega g(\eta\ ,\tau)$$
$$w = -4(\nu\Omega)^{1/2} h(\eta\ ,\tau),\quad \frac{T-T_\infty}{T_w-T_\infty} = \theta(\eta\ ,\tau)$$
$$\eta = \frac{1}{2}\sqrt{\left(\frac{\Omega}{\nu}\right)}z,\ \tau = \Omega t,\quad p = 2\rho_\infty \nu\Omega\bar{p}(\eta,\tau) \quad (37)$$

Hence, the governing equations (1) to (5) reduce to the following forms, after using the transformation as exhibited in (37):

$$(1+\varepsilon\theta)h''' - \varepsilon\theta' h'' + (1+\varepsilon\theta)^2\left(4g^2 + 8h''h - 4h'^2\right) = 0 \quad (38)$$

$$(1+\varepsilon\theta)g'' - \varepsilon\theta' g' + (1+\varepsilon\theta)^2\left(8hg' - 8h'g\right) = 0 \quad (39)$$

$$\bar{p}' = (1+\varepsilon\theta)^{-1}h'' - 2\varepsilon(1+\varepsilon\theta)^{-2}\theta' h' + 8hh' \quad (40)$$

$$\theta'' + 8\,Pr\,\theta'\,h = 0 \quad (41)$$

and the corresponding boundary conditions take the following forms:

$$h(0) = h'(0) = 0,\ g(0) = 1,\ \theta(0) = 1$$
$$h'(\infty) = g(\infty) = \theta(\infty) = \bar{p}(\infty) = 0 \quad (42)$$

To find the solutions to the above sets of equations, we have applied the same method as used in the preceding section. As before, once the values of the functions h, g, and θ along with their derivatives are known, we can easily find the values of dimensionless radial-skin friction, tangential skin-friction, as well as heat transfer rate, using the large τ limit from equation (16) as presented below:

$$\bar{\tau}_r(1+\varepsilon) = h''(0), \bar{\tau}_t(1+\varepsilon) = g'(0)$$
$$\bar{q} = -\theta'(0) \quad (43)$$

In this section, it is worth pointing out that the equations (38) to (41) reduce to the same equations as those investigated by Benton [III], Sparrow and Gregg [IV], and Hartnett [X] when the viscosity of fluid was treated as constant which corresponds to ε = 0.0, the viscosity variation parameter in this study. However, the values of the dimensionless radial skin friction, $\bar{\tau}_r(1+\varepsilon)$ and tangential skin friction, $\bar{\tau}_t(1+\varepsilon)$ and heat transfer rate, $\bar{q}$, are estimated from our present numerical simulation, and these results are presented in the tabular form to compare our results with the available results obtained by other researchers as well as to compare our results obtained by different methods in this study for different pertinent parameters.

VI. Results and discussion

The three-dimensional and transient numerical simulations have been performed employing distinct solution methodologies for different τ limits, for example, small-time regime, large-time regime, and all-time regime as discussed in the previous sections to reveal the effect of temperature dependent viscosity variation parameter, ε on the fluid flow behavior, and heat transfer processes due to an impulsively started rotating disc. In this study, we have considered the different values of the Prandtl number (*Pr*) such as *Pr* = 0.72 (suitable for air) and *Pr* = 0.10, 0.05, and 0.02 (appropriate for the liquid metals) while the viscosity variation parameters are ε = 0.0 and 1.0. The results of physical interest which are computed in this study numerically include the non-dimensional local radial skin-friction, tangential skin-friction, and the rate of heat transfer at the surface of the rotating disc against the time-dependent parameter, τ, and hence, these results have been shown in tables 1 to 4 respectively.

Table:1

Numerical values of the tangential skin-friction coefficients, $(1+\varepsilon)\bar{\tau}_t$ obtained for *Pr* = 0.72 while ε = 0.0			
	Benton [III]	Present	
τ	Series solution		Finite difference solution
0.10	3.57300s	3.57959s	3.57957
0.20	2.53907s	2.54370s	2.54360
0.40	1.83047s	1.83366s	1.83349
0.60	1.54086s	1.54334s	1.54323
0.80	1.38790s	1.38992s	1.39018
1.00	1.29881s	1.30050s	1.30189
2.00			1.18990
3.00			1.20256
4.00			1.21734
5.00			1.22494
∞	1.231844*a*	1.23192*a*	1.23127

Here, '*s*' for small τ, and '*a*' for asymptotic τ.

We have demonstrated the solutions of the perturbation technique for small τ and the asymptotic solutions for large τ along with the finite difference solutions for the entire τ-regime in *tables* 1 to 4, and we have also presented these results graphically in *figures*

2a to 2c for comparisons. It is worth mentioning here that in these tables, the numerical values marked by '*s*' represent those values that are obtained by perturbation solution techniques for a small time, and the values which are indicated by '*a*' are obtained for a large time i.e., asymptotic solutions (in other words, steady-state solutions). It is apparent that the comparisons of the aforesaid solutions with the finite difference solutions (i.e., all time regime) show excellent agreement in the respective regimes, i.e., in the small- and large-time regimes. It should be mentioned here that in *figures* 2a to 2c, the dashed and dashed-dot curves represent, respectively the solutions obtained for small and large τ, and the solid lines represent the finite difference solutions for the entire τ-regime. Hence, one can easily conclude that the comparison between the dashed and the dashed-dotted curves with the solid lines again shows excellent agreement.

Table 2

From *table 1*, it is seen that the values of the tangential skin friction at the surface of the disc decrease with increasing τ, the time-dependent rotating parameter, for uniform viscosity (i.e., ε = 0.0) and *Pr* = 0.72. The computed values of the aforesaid quantity

Numerical values of the radial skin-friction coefficients, $(1+\varepsilon)\bar{\tau}_r$ obtained by different methods for different Pr while ε = 1.0						
τ	*Pr* = 0.10		*Pr* = 0.05		*Pr* = 0.02	
	Series	Finite	Series	Finite	Series	Finite
0.05	0.25808s	0.25795	0.25838s	0.25833	0.25859s	0.25863
0.10	0.36481s	0.36427	0.36523s	0.36492	0.36554s	0.36544
0.20	0.52498s	0.52332	0.51577s	0.51451	0.51600s	0.51549
0.40	0.72305s	0.71872	0.72386s	0.72096	0.72444s	0.72291
0.60	0.87522s	0.86822	0.87615s	0.87138	0.87682s	0.87426
0.80	0.99479s	0.98538	0.99567s	0.98927	0.99646s	0.99294
1.00	1.09110s	1.07945	1.09208s	1.08384	1.09277s	1.08815
2.0	1.39669s	1.33718	1.39788s	1.34146	1.39873s	1.34652
3.0		1.41651		1.41936		1.42307
4.0		1.43716		1.43911		1.44140
5.0		1.44180		1.44329		1.44463
∞	1.44281*a*	1.44365	1.44222*a*	1.44358	1.44025*a*	1.44354

Here, '*s*' for small τ, and '*a*' for asymptotic τ.

is in excellent agreement with the corresponding results as obtained by Benton [III] which is presented in the preceding section.

It is seen from *Table* 2 that the value of the local radial skin friction at the surface of the rotating disc increases with the increasing value of τ until the asymptotic value for the steady-state flow limit is reached, at each given value of the Prandtl number (*Pr*).

The opposite scenario is seen, in *tables* 3 and 4, in the case of the tangential skin friction, and heat transfer rate at the surface of the disc. Besides, one can further observe from the above-mentioned *tables* that the value of the radial skin friction increases, whereas the tangential component of the skin friction as well as the heat transfer rate decrease with a decrease in the value of Prandtl number (*Pr*) in the entire flow regime.

Table: 3

Numerical values of the tangential skin-friction coefficients, $(1+\varepsilon)\bar{\tau}_t$ obtained by different methods for different *Pr* while ε = 1.0

τ	*Pr* = 0.10		*Pr* = 0.05		*Pr* = 0.02	
	Series	Finite	Series	Finite	Series	Finite
0.05	7.32714s	7.34325	7.27105s	7.28325	7.22612s	7.23492
0.10	5.28732s	5.20628	5.14767s	5.16193	5.11591s	5.12558
0.20	3.68561s	3.70951	3.65760s	3.67474	3.63517s	3.64613
0.30	3.03308s	3.05951	3.01026s	3.02909	2.99198s	3.00401
0.40	2.65526s	2.68307	2.63554s	2.65533	2.61975s	2.63226
0.50	2.40726s	2.43570	2.38967s	2.40992	2.37559s	2.38832
0.60	2.23289s	2.26145	2.21688s	2.23727	2.20408s	2.21685
0.70	2.10506s	2.13341	2.09029s	2.11061	2.07848s	2.09123
0.80	2.00877s	2.03675	1.99500s	2.01519	1.98400s	1.99676
0.90	1.93489s	1.96249	1.92194s	1.94209	1.91160s	1.92454
1.00	1.87741s	1.90483	1.86516s	1.88550	1.85538s	1.86880
2.0	1.63088s	1.72153	1.62135s	1.70978	1.61384s	1.69993
3.0		1.72822		1.71965		1.71378
4.0		1.74497		1.73760		1.73365
5.0		1.75397		1.74728		1.74421
∞	1.76386*a*	1.75938	1.75607*a*	1.75568	1.76115*a*	1.75366

Here, '*s*' for small τ, and '*a*' for asymptotic τ.

Table: 4

Numerical values of the rate of heat transfer, $\bar{q}$ obtained by different methods for different Pr while ε = 1.0

τ	*Pr* = 0.10		*Pr* = 0.05		*Pr* = 0.02	
	Series	Finite	Series	Finite	Series	Finite
0.05	1.60065s	1.60052	1.13358s	1.13354	0.74585s	0.74731
0.10	1.13210s	1.13358	0.80171s	0.80170	0.52746s	0.52961
0.20	0.80125s	0.80108	0.56730s	0.56733	0.37316s	0.37367
0.40	0.56863s	0.56839	0.40299s	0.40239	0.26439s	0.26939
0.60	0.46702s	0.46671	0.32999s	0.33017	0.21656s	0.22326
0.80	0.40764s	0.40726	0.28754s	0.28784	0.18834s	0.19673
1.00	0.36808s	0.36764	0.25909s	0.25955	0.16931s	0.17940
2.0	0.27449s	0.27613	0.19063s	0.19400	0.12284s	0.14211
3.0		0.24038		0.16907		0.13011
4.0		0.22036		0.15626		0.12457
5.0		0.20713		0.14872		0.12140
∞	0.16572*a*	0.16588	0.13015*a*	0.13109	0.11257*a*	0.11202

Here, '*s*' for small τ, and '*a*' for asymptotic τ.

The influence of the viscosity-variation parameter, ε (= 0.0, 2.0, 4.0 and 6.0), on the dimensionless radial skin-friction, tangential skin-friction, and the rate of heat transfer for the fluid with *Pr* = 0.72 are presented graphically, respectively, in *figures* 2a to 2c.

From *figures* 2a and 2b, it is clearly seen that an increase in the values of ε, the viscosity variation parameter, leads to an increase in both values of local radial skin-friction and local tangential skin-friction. However, the increasing values of τ cause an increase in the values of local radial skin-friction and decrease in the values of local tangential skin-friction until their asymptotic values are achieved.

Finally, from *figure* 2c, it is found that the values of heat transfer rate decrease owing to an increase in the values of ε until the steady-state situations are achieved.

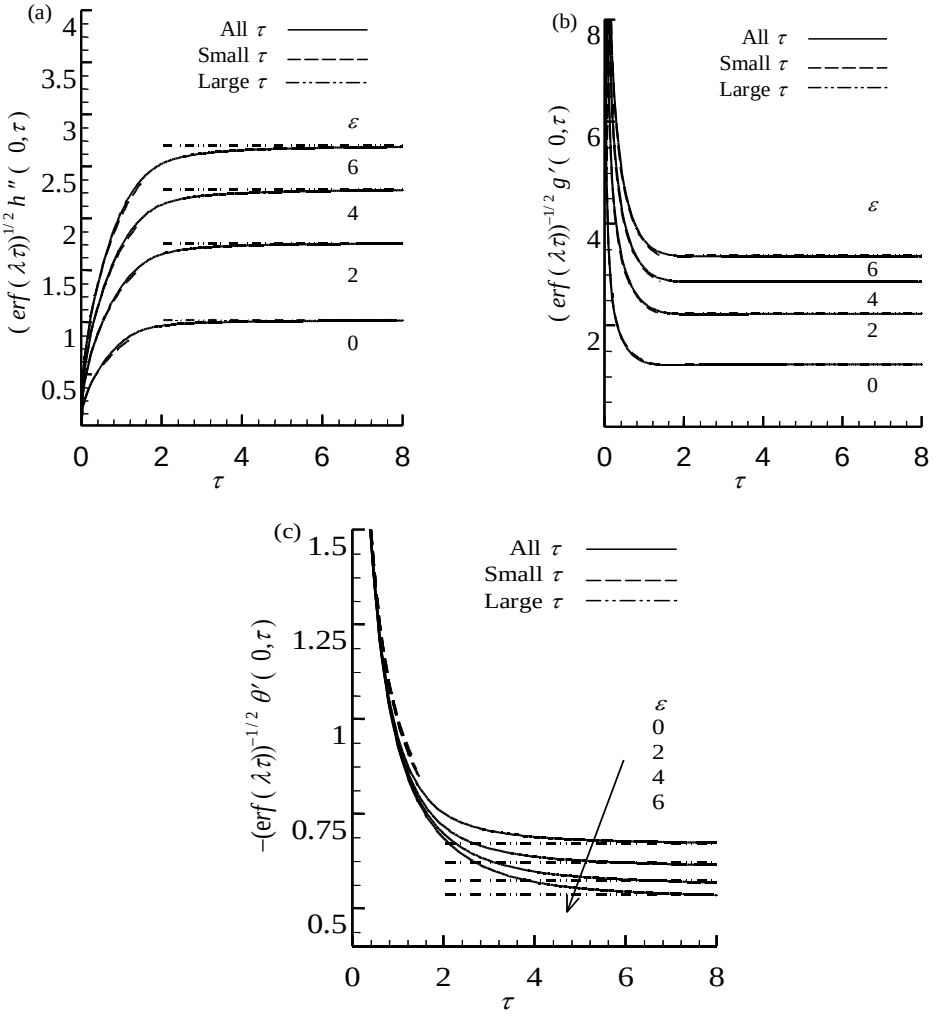

Fig. 2 (a) The non dimensional radial skin-friction, $(1+\varepsilon)\bar{\tau}_r$, (b) tangential skin-friction, $(1+\varepsilon)\bar{\tau}_t$, and (c) rate of heat transfer, $\bar{q}$ against τ, for different values of ε with *Pr* = 0.72.

More importantly, it is observed that there are significant effects of ε on the rate of heat transfer in the region $\tau \geq 1.0$ (approximately).

The effect of an increase in the values of the viscosity-variation parameter, ε (= 0.0, 2.0,4.0,6.0 and 8.0), on the dimensionless velocity and temperature profiles against η, for the fluid with Prandtl number *Pr* equal to 0.72 are presented in *figures* 3a to 3d. It is found in *figures* 3a to 3c that an increase in the values of ε leads to a decrease in the

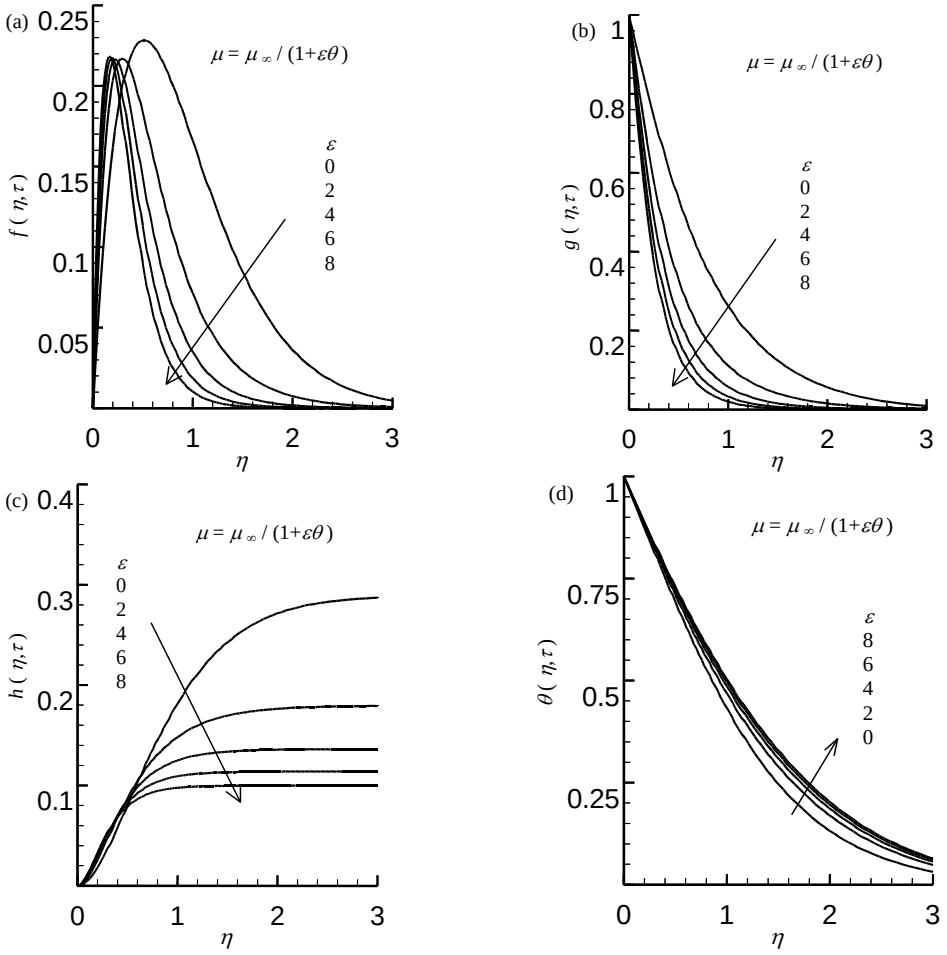

Fig. 3 (a) The dimensionless radial velocity profile, $f(\eta,\tau)$, (b) tangential velocity profile, $g(\eta,\tau)$, (c) axial velocity profile, $h(\eta,\tau)$, and (d) temperature profile, $\theta(\eta,\tau)$ against η for different values of ε, with Pr = 0.72.

values of dimensionless radial, tangential and axial velocity profiles and this significant effect eventually leads to a decrease in the momentum boundary layer thickness.

From *figure* 3d, it is found that values of non-dimensional temperature increase with increasing values of ε, and this effect ultimately leads to a small rate of increase in the thermal boundary layer thickness. Since the radial velocity is zero at the disc

surface and in the ambient fluid, there must be a maximum value of it somewhere in between the zones as mentioned above, and this maximum will be positive as the radial flow is always outwards along the disc. Figure 3a shows that the point of maximum radial velocity for uniform viscosity, i.e., ε = 0.0, appears at $\eta \approx 0.52$. As the viscosity variation parameter, ε increases, the point of maximum velocity moves closer to the surface of the rotating disc.

VII. Concluding Remarks

In this paper, the influence of temperature-dependent viscosity on the transient flow of an incompressible fluid and heat transfer processes, due to an impulsively started rotating disc in a three-dimensional cylindrical coordinate system, has been investigated numerically by employing an in-house numerical code. The governing equations for the unsteady flow and heat transfer processes are converted to a set of local non-similarity equations with the help of a newly developed and appropriate set of transformations which are valid for a small time and large time regimes as well as in the entire time regime. Subsequently, to demonstrate the accuracy of our numerical solutions for different τ limits, the three different solution methods have been applied for obtaining the numerical solutions of the resulting non-similarity equations, such as (i) perturbation solutions for small-time, (ii) asymptotic solutions for large time, and (iii) implicit finite difference methods for the entire time with the Keller-Box [VIII] elimination technique. However, from our present investigation, we can summarize our major findings as follows:

1. The solutions which have been computed numerically in this study for small τ limit and large τ limit are found in excellent agreement with that the results obtained for the entire τ limit at any value of the Prandtl number, *Pr* [= 0.10, 0.05, and 0.02] while ε = 1.0. Besides, the similar scenarios are observed for the viscosity variation parameter, ε, equals 0.0, 2.0, 4.0, and 6.0 for the fixed Prandtl number, *Pr* = 0.72.
2. The local radial skin-friction increases at the disc surface for different values of *Pr* = 0.10, 0.05, and 0.02 when ε =1.0 is kept constant, whereas the local tangential skin-friction and the rate of heat transfer decrease with the increasing values of τ. The same behavior is observed for the above-mentioned quantities as the Prandtl number, *Pr*, decreases at the entire τ-limit.
3. For a given value of *Pr*, the local radial skin friction and tangential skin friction are increased due to an increase in the value of the viscosity variation parameter, ε. The local heat transfer rate decreases due to an increase in the viscosity-variation parameter, ε, and more remarkable effects of ε on the heat transfer rate are found in the regime of $\tau \geq 1.0$.
4. For *Pr* equals 0.72, it is observed that the dimensionless radial, tangential and axial velocity profiles decrease due to the increase in the values of ε, which eventually leads to a decrease in the thickness of the momentum boundary layer. Besides, the non-dimensional temperature profile increases when the value of ε increases, and consequently, this effect gives rise to a slight increment in the thermal boundary layer thickness.

Although the present study is limited to the regime of laminar boundary layer flow and heat transfer due to the fact of the uniform angular velocity of the rotating disc, the present work can be extended to the regime of turbulent boundary layer flow along with the heat transfer processes by increasing the angular velocity of the rotating disc. The thermal status can be treated directly by the modelling of combustion or burning process over the surface of the disc adopting an overall chemical reaction scheme by which the rotating disc surface wall will be heated automatically in a variable manner instead of using the traditional method, that is the 'prescribed temperature field' at the surface of the disc. This work is at present under progress, which will be reported soon somewhere else.

Conflict of Interest: There are no conflicts of interest regarding the publication of this research article.

References:

I. A. Mehmood, M. Usman, Heat transfer enhancement in rotating disk boundary-layer, Thermal Sciences, vol. 22 pp: 2467-248, 2018.

II. A. Nilankush, B. Raju, P. K. Kundu, Influence of hall current on radiative nanofluid flow over a spinning disk: a hybrid approach, Physica E: Low dimensional systems and nanostructures, vol. 111, pp: 103-112, 2019.

III. E. R. Benton, On the flow due to a rotating disc, Journal of Fluid Mechanics, vol. 24, pp: 781- 800, 1966.

IV. E. M. Sparrow, J. L. Gregg, Heat transfers from a rotating disk to a fluid of any Prandtl number, ASME Journal of Heat Transfer, vol. 81, pp: 249-251, 1959.

V. F. Kreith, Convection heat transfer in rotating systems, Advances in Heat Transfer, vol. 5, pp:129–251, 1969.

VI. G. K. Batchelor, Note on a class of solutions of the Navier-Stokes equations representing steady non-rotationally symmetric flow, The Quarterly Journal of Mechanics and Applied Mathematics, vol. 4, pp. 29-41, 1951.

VII. H. Ockendon, An asymptotic solution for steady flow above an infinite rotating disc with suction, The Quarterly Journal of Mechanics and Applied Mathematics, vol. 25, pp: 291-301, 1972.

VIII. H. B. Keller, Numerical methods in the boundary layer theory, Annual Annual Review of Fluid Mechanics, vol. 10, pp: 417-433, 1978.

IX. I. V. Shevchuk, Convective heat and mass transfer in rotating disk systems, Lecture Notes in Applied and Computational Mechanics, vol. 45, Springer-Verlag Berlin Heidelberg, 2009.

X. J. P. Hartnett, Heat transfer from a non-isothermal rotating disc in still air, ASME Journal of Applied Mechanics, vol. 26, no. 4, pp: 672-673, 1959.

XI. J. T. Stuart, On the effect of uniform suction on the steady flow due to a rotating disc, The Quarterly Journal of Mechanics and Applied Mathematics, vol. 7, pp: 446-457, 1954.

XII. J. C. Butcher, Implicit Rungee-Kutta process, Journal of Mathematics of Computation, vol. 18, no. 85, pp. 50-64,1964.

XIII. J. M. Owen, R. H. Rogers, Flow and heat transfer in rotating disc systems: Rotor-stator systems, Research Studies, Taunton, U.K. and John Wiley, NY, USA, 1989.

XIV. J. F. Brady, L. Durlofsky, On rotating disk flow, Journal of Fluid Mechanics, vol. 175, pp: 363-394, 1987.

XV. J. X. Ling, A. Dybbs, Forced convection flow over a flat plate submerged in a porous medium with variable viscosity case, Conference of ASME, paper no. 87- WA/TH-23, New York, 1987.

XVI. J. Herrero, J. A. C. Humphrey, F. Giralt, Comparative analysis of coupled flow and heat transfer between co-rotating discs in rotating and fixed cylindrical enclosures, ASME Heat Transfer Division, vol. 300, pp: 111-121, 1994.

XVII. M. G. Rogers, G. N. Lance, The rotationally symmetric flow of a viscous fluid in presence of infinite rotating disc, Journal of Fluid Mechanics, vol. 7, pp: 617-631, 1960.

XVIII. M. A. Hossain, S. M. Munir, Mixed convection flow from a vertical flat plate with temperature dependent viscosity, International Journal of Thermal Sciences, vol. 39, no. 2, pp: 173-183, 2000.

XIX. M. A. Hossain, A. Hossain, M. Wilson, Unsteady flow of viscous incompressible fluid with temperature-dependent viscosity due to a rotating disc in presence of transverse magnetic field and heat transfer, International Journal of Thermal Sciences, vol. 40, no. 1, pp: 11-20, 2001.

XX. M. A. Hossain, S. Kabir, D. A. S. Rees, Natural convection of fluid with variable viscosity from a heated vertical wavy surface, Journal of Applied Mathematics and Physics, Vol. 53 pp: 48-52, 2002.

XXI. M. M. Awad, Heat transfer from a rotating disk to fluids for a wide range of Prandtl numbers using the asymptotic model, ASME Journal Heat Transfer, vol. 130, no.014505, pp: 1-4, 2008.

XXII MD. Shamshuddin, S. R. Mishra, O. A. Bég, A. Kadir, Numerical study of heat transfer and viscous flow in a dual rotating extendable disk system with a non-Fourier heat flux model, Heat Transfer Asian Research, vol. 48, pp: 1-25, 2018.

XXIII. M. Ibrahim, Numerical analysis of time-dependent flow of viscous fluid due to a stretchable rotating disk with heat and mass transfer, Results in Physics, vol. 18 , no. 103242, pp:1-6, 2020.

XXIV. M. Ramzan, N. S. Khan, P. Kumam, A numerical study of chemical reaction in a nanofluid flow due to rotating disk in the presence of magnetic field, Scientific Reports, vol. 11, no. 19399, pp:1-24, 2021.

XXV. N. G. Kafoussias, D. A. S. Rees, J. E. Daskalakis, Numerical study of the combined free and forced convective laminar boundary layer flow past a vertical isothermal flat plate with temperature dependent viscosity, Acta Mechanica, vol. 127, pp: 39-50, 1998.

XXVI. P. R. Nachtshiem, P. Swigert, Satisfaction of the asymptotic boundary conditions in numerical solution of the system of non-linear equations of boundary layer type, NASA TND-3004, 1965.

XXVII. P. R. N. Childs, Rotating flow, 1st Edition, Butterworth–Heinemann, UK, 2010.

XXVIII. S. Ostrach, P. R. Thorton, Compressible laminar flow and heat transfer about a rotating isothermal disc, NACA Technical Note 4320, 1958.

XXIX S. P. Anjali Devi1, R. Uma Devi, On hydromagnetic flow due to a rotating disk with radiation effect, Nonlinear Analysis: Modelling and Control, vol. 16, pp: 17–29, 2011.

XXX. S. Imayama, P. H. Alfredsson, R. J. Lingwood, Experimental study of rotating-disk boundary-layer flow with surface roughness, Journal of Fluid Mechanics, vol. 786, no. 5, pp:5-28, 2016.

XXXI. T. Von Ka′rma′n, Üeber laminare und turbulente reibung, ZAMM, vol. 4, pp: 233-252, 1921.

XXXII. T. Cebeci, P. Bradshaw, Physical and computational aspects of convective heat transfer, Springer-Verlag, New-York, 1984.

XXXIII. T. Hayat, M. Ijaz Khan, A. Alsaedi, M. Imran Khan, Joule heating and viscous dissipation in flow of nanomaterial by a rotating disk, International Communications in Heat Mass Transfer, vol. 89, pp: 190-197, 2017.

XXXIV. U. T. Bödewat, Die drehströmung üeber festem grunde, ZAMM, vol. 20 , pp: 241-253, 1940.

XXXV. W. G. Cochran, The flow due to a rotating disc, Proceedings of the Cambridge Philosophical Society, vol.30, pp.365-37, 1934.